Physics – Uspekhi **49** (4) 353 – 368 (2006)

REVIEWS OF TOPICAL PROBLEMS PACS numbers: **73.21.–b**, **73.22.–f**, 73.43.Lp, **78.67.–u**

Inelastic light scattering spectroscopy of electron systems in single and double quantum wells

L V Kulik, V E Kirpichev

DOI: 10.1070/PU2006v049n04ABEH005885

Contents

Abstract. Inelastic light scattering is used to study the spectra of neutral excitations and magnetoexcitations in single and double quantum wells. New excitation branches of charge, spin, and charge–spin densities are observed. It is shown that various electron and phonon excitation modes interact with one another to form hybrid modes. Exchange and correlation corrections for the combined resonance energies in the integer and fractional Hall effects are estimated. The effect of a spatial inversion asymmetry on the excitation spectra of single-particle and collective excitations is considered.

1. Introduction

The interpretation of elementary excitations as quasiparticles suggested by Landau in 1941 [1] offers an effective method for the description of physical properties of multielectron systems. It is postulated in the quasiparticle theory that electrons or quasielectrons in the p-space fill the same volume of radius p_F as free electrons, while excitation states are described by weakly interacting quasiparticles with charges $-e$ and $+e$, spin 1/2, and corresponding effective masses and lifetimes. The concept of quasiparticles allows reducing the complex dynamics of a system to simple dynamics of a totality of quasi-independent objects. Practically speaking, the problem may be reduced to the consideration of a gas-like system; such an approach allows equilibrium and nonequilibrium systems with strong interactions to be described by relatively simple methods of statistical thermodynamics and kinetics of gases.

Elementary excitations are categorized into single-particle and collective. Single-particle excitations in an electron system may be likened to an elementary act in which an electron inside the Fermi sphere acquires an additional momentum q and passes from a state with momentum p to one of the free states with momentum p' outside the sphere. Collective excitations are exemplified by plasma excitations. In the simplest theory of plasma excitations developed by Bohm and Pines [2], positive ions of a solid are substituted by a uniformly distributed positive charge or 'gel' with the density equalling the average charge density of the electrons. Conduction electrons with an effective mass m^* are regarded as a gas of a mean density n whose rarification and compression cause longitudinal oscillations. These oscillations are due to Coulomb interactions between electrons and the positively charged ion backbone; they are referred to as plasma waves and their quanta as plasmons.

The plasmon dispersion law is given by

$$\omega^2(q) = \omega_p^2 + \frac{\gamma}{m^* n}\, q^2 , \qquad (1)$$

where $\omega_p^2 = 4\pi e^2 n/\varepsilon m^*$ is the squared plasma frequency, γ is the elasticity modulus of an electron gas regardless of charges, and ε is the dielectric permittivity. At $e \to 0$, electrostatic effects vanish and $\omega(q) \approx q(\gamma/m^* n)^{1/2}$. This dependence coincides with the dispersion law for sound waves that propagate in a gas with the speed $(\gamma/m^* n)^{1/2}$. Usually,

L V Kulik, V E Kirpichev Institute of Solid State Physics,
Russian Academy of Sciences,
142432 Chernogolovka, Moscow region, Russian Federation
Tel. (7-496) 522 25 72
Fax (7-496) 524 97 01
E-mail: kulik@issp.ac.ru, kirpich@issp.ac.ru

Received 6 September 2005, revised 11 October 2005
Uspekhi Fizicheskikh Nauk **176** (4) 365 – 382 (2006)
Translated by Yu V Morozov; edited by A M Semikhatov

$\omega_p \gg q(\gamma/m^*n)^{1/2}$ and the dispersion of plasma waves is insignificant.

The concept of quasiparticles is successfully applied to the description of spatially anisotropic multielectron systems composed of electrons at the surface of liquid helium, silicon MIS structures, and semiconducting heterostructures with quantum wells. The motion of such systems is possible only in one spatial direction because of the splitting of their energy spectrum into a set of dimensional quantization subbands.

When energy scales related to transverse quantization exceed all other characteristic energies (the Fermi energy and the thermal energy), the electron system becomes two-dimensional (2D) and its density of states constant, depending on the electron effective mass alone. The excitation spectrum of a 2D electron system displays a number of unique properties. Specifically, new excitation branches are observed, some in the lowest dimensionally quantized subband (intrasubband or proper two-dimensional excitations) and others with an altered subband index (intersubband excitations). Both intra- and intersubband excitations can be single-particle or collective.

Intrasubband excitations or plasma waves were first described in 1967 [3]. Their dispersion in the longwave limit ($m^*\omega \gg qk_F$) is determined by

$$q^2 = \frac{\varepsilon\omega^2}{c^2} + \left(\frac{\omega^2}{2\pi e^2 N/m^*\varepsilon}\right)^2, \qquad (2)$$

where N is the electron surface density. At $q \gg 2\pi e^2 N/m^* c^2$, the first term on the right-hand side of Eqn (2) is small and the plasmon dispersion becomes root-like:

$$\omega^2(q) = \frac{2\pi e^2 qN}{\varepsilon m^*}. \qquad (3)$$

At $q < 2\pi e^2 N/m^* c^2$, the second term on the right-hand side of (2) may be neglected and $q \approx \sqrt{\varepsilon}\,\omega/c$, which corresponds to the light-wave dispersion in a medium with the refractive index $\sqrt{\varepsilon}$.

Plasma wave dispersion changes from root to linear when the phase velocity of the waves approaches the speed of light (the delay effect). For the typical parameters of heterostructures, it occurs at $q = 10$ cm^{-1} and the frequency 10 – 30 GHz. A few years ago, 2D plasmons could not be observed at such low frequencies, the linewidth of plasma resonance being some 1000 GHz because of the poor quality of the study structures. The quality of samples has been improved substantially in recent years. The mobility of two-dimensional electrons has increased by several orders of magnitude and the linewidth of plasma resonance has decreased to 1 – 3 GHz. GaAs/GaAs-based heterostructures exhibit weakly damping hybrid plasmon – polariton modes (light-bound plasmon states), whose energy is described by formula (2) [4].

We note that expression (2) was derived on the assumption that the plane occupied by the electron system is located in a homogeneous medium with a uniform dielectric permittivity. In a real situation, however, the picture may be more complicated. For example, in the case of silicon MIS structures, electrons forming the inversion layer in a semiconductor lie between the dielectric layer adjacent to the metal gate and the spatial charge layer adjoining the bulk semiconductor. Metal electrodes can also be found in the immediate proximity to the electron system at the liquid helium surface. The presence of conducting boundaries changes the dispersion ratio for a plasmon [5]. The metal electrodes screen Coulomb interactions, thus softening the plasmon frequency; in the longwave limit, the plasmon dispersion becomes linear [6 – 8].

Application of an external magnetic field oriented normally to the plane of a 2D system results in the quantization of electron motion in this plane while the energy spectrum becomes totally discrete. The density of states is a set of δ-functions (Landau levels) separated by the cyclotron energy. Filling of the Landau levels with electrons is characterized by a filling factor ν defined as the ratio of the electron density to the multiplicity of degeneracy per unit area. In real 2D systems, the Landau levels acquire a finite width due to the interaction of electrons with a random potential and the distribution of the single-particle density of states is determined by the character of inhomogeneities [9].

The appearance of gaps in the electron state density leads to fundamental macroscopic phenomena such as the integer and fractional quantum Hall effects (QHEs) [10, 11]. We recall that the integer QHE consists in the fact that at roughly integer-valued filling factors, the longitudinal tensor component vanishes and the transverse (Hall) one is quantized. These events can be accounted for by the fact that the conductivity of a 2D system is a topological invariant independent of the properties of the random impurity potential.

In the fractional QHE, the Hall conductivity is quantized at fractional values of filling factors due to the formation of incompressible quantum liquids in the ground state of a given electron system that are separated from the excited states by energy gaps [12 – 14]. A theory describing the fractional QHE as an integer one, not for electrons but for new quasiparticles, composite fermions that are bound states of electrons and an integer number of magnetic field quanta, has become popular in recent years. Fractional QHE states of electrons with the filling factor $\nu = p/(2np \pm 1)$ correspond to integer QHE states of composite fermions with the filling factor $\nu^* = p$, whereas composite fermions themselves move in the effective magnetic field $B_{\text{eff}} = B - B_{1/2n}$, where $B_{1/2n}$ is the magnetic field at $\nu = 1/2n$ [15 – 18].

Excitations of a 2D electron system in a magnetic field are represented by magnetoexcitons and magnetoplasmons, i.e., bound states of a hole at a filled level with a number n and of an electron at one of the vacant Landau levels with a number n' [19]. The Hamiltonian of a magnetoexciton is translationally invariant, and the corresponding integral of motion is the generalized momentum, all of whose components commute with each other:

$$\mathbf{k} = -\mathrm{i}\,(\nabla_1 + \nabla_2) + \frac{e}{c}\,(\mathbf{A}_1 - \mathbf{A}_2) - \frac{e}{c}\left[(\mathbf{r}_2 - \mathbf{r}_1) \times \mathbf{B}\right], \quad (4)$$

where $\hbar = 1$, the respective indices 1 and 2 denote negatively and positively charged particles, and $\mathbf{A}_1$ and $\mathbf{A}_2$ are vector potentials [20 – 22].

Excitations in a magnetic field are classified in terms of the dispersion dependences on the generalized momentum. At $\omega_c \gg e^2/\varepsilon l_B$, the function

$$E_m(\mathbf{k}) = m\omega_c + g\mu_B BS_z + \Delta E_m(\mathbf{k}), \qquad (5)$$

where $m = n' - n$ is a nonnegative integer, ω_c is the cyclotron frequency, $l_B = (c/eB)^{1/2}$ is the magnetic length, $g\mu_B BS_z$ is

the Zeeman splitting energy for spin-flip transitions, and $\Delta E_m(\mathbf{k})$ is a function given by the Coulomb interaction. The function $\Delta E_m(\mathbf{k})$ depends on m and on the initially filled Landau level; moreover, in the general case, a few ΔE_m branches may exist and additional indices must be introduced to distinguish them.

Low-energy excitations with $m = 0, 1$ are the most interesting ones. When both spin sublevels of the Landau levels with the indices $n = 0, 1, \ldots, \nu_0 - 1$ are filled, the ground state is characterized by an eigenfunction with the spin number $S = 0$, and excitations with $m = 1$ may be classified as singlets or triplets.

The singlet branch is a magnetoplasmon with the linear longwave dispersion ($ql_B \ll 1$)

$$E(\mathbf{k}) = \omega_c + \alpha k\,, \tag{6}$$

which assumes the known classical form in small fields:

$$E(k) = \left(\omega_c^2 + \omega_p^2(q)\right)^{1/2}, \tag{7}$$

where $\omega_p(q)$ is the plasma frequency without the magnetic field with the momentum $q = k$. Triplet excitations with $S = 1$, $S_z = 0, \pm 1$ have energies given by the cyclotron energy $S_z = 0$ and shifted relative to it by the Zeeman energy $g\mu_B B\,\delta S_z$ ($S_z = \pm 1$). The longwave dispersion of a triplet magnetoexciton is quadratic.

In the case of differentially filled spin sublevels, the excited states cannot be divided into singlet or triplet ones. If $\nu_\downarrow = \nu_\uparrow + 1$, where $\nu_\downarrow$ and $\nu_\uparrow$ are the respective numbers of the filled Landau levels for the downward and upward spins, and $\nu_\uparrow > 0$, the excitation spectrum with $m = 1$ contains two plasma modes. In the longwave limit, one of them has magnetoplasmon dispersion (6) and the other is characterized by a quadratic dispersion. There is also a spin-flip mode, i.e., the electron excitation with a spin flip. When only one spin sublevel of the lowest Landau level $\nu_\uparrow = 0$ is filled, there is a single plasma mode (6) and a single spin-flip mode. In the longwave limit, the spin-flip mode has an energy much in excess of the cyclotron energy, due to the difference in the exchange energies at the zeroth and the first Landau levels [23].

In all these cases, the excitation branch with $m = 1$ and $\delta S_z = 0$ has the energy $E(\mathbf{k}) \to \omega_c$ as $k \to 0$, and the Kohn theorem [24] holds, claiming that electron–electron interactions have no effect on the cyclotron resonance energy in a spatially uniform system. As regards excitations with $\delta S_z = +1, -1$, their energies at $k \to 0$ may be shifted with respect to the cyclotron energy by the exchange energy value. In the absence of scattering on the alloy potential, longwave excitations with $m = 1$, $\delta S_z = 0$ have an infinite lifetime because the system can have no other states with the same energy, generalized momentum, and spin quantum number. Excitations with $\delta S_z = +1, -1$ may decay into a spin exciton with $m = 0$, $\delta S_z = 1$ and a magnetoplasmon with $m = 1$, $\delta S_z = 0$.

There are no excitations with $m = 0$ when an equal number of Landau spin sublevels are filled. Otherwise, the spectrum shows spin-flip excitations, i.e., spin excitons or magnons. In the quantum ferromagnetic state $\nu_\downarrow = 1, \nu_\uparrow = 0$, the longwave magnon dispersion is quadratic,

$$E_0(\mathbf{k}) - g\mu_B B \sim k^2\,,$$

while in the shortwave limit, it is described by a constant given by the exchange energy at the zeroth Landau level. Also, there are excitations in the shortwave limit, whose energy is smaller than the magnon energy. These are skyrmion–antiskyrmion pairs [25]. A skyrmion with the energy $E_S = (1/4)\,E_0(\infty)$ is a topological excitation over the vector field of electron spins, and the energy of a skyrmion–antiskyrmion pair is lower than the energy of a shortwave magnon. Despite extensive literature on the theory of skyrmion excitations [26], no direct experimental observation of skyrmions has thus far been reported. This can be accounted for by the fact that the electrons in the 2D systems being studied have a large effective g-factor. The value of δS_z in skyrmion excitations being high, the loss of the Zeeman energy by an excited skyrmion–antiskyrmion pair is not compensated by the gain of the exchange energy.

Excitations with $m = 0$ without spin flip are 'magnetophonons' or electron excitations inside partially filled Landau levels in fractional QHE states. Having a roton minimum, these excitations resemble phonons in superfluid helium. The shortwave gap on the magnetophonon dispersion curve is due to the excitation of a pair of charged quasiparticles formed by a quasielectron with a fractional charge $-\nu$ and a quasihole with the fractional charge ν. The size of the gap in this region is easy to deduce from the measurement of the activation energy in dissipative conductivity [27]. The most difficult for experimental analysis is the section of the dispersion curve with small momenta and momenta of the order of the inverse magnetic length, where the dispersion has a roton minimum. A few characteristic points at the dispersion curve of the magnetophonon mode at $\nu = 1/3$ were obtained by inelastic light scattering spectroscopy [28].

Recently, a new line of 2D-system research has emerged, focused on electron systems with spatial charge separation or double electron layers. The physical realization of double layers is a semiconducting heterostructure with two symmetrically alloyed quantum wells (DQWs) separated by a narrow potential barrier. The presence of two layers in DQWs gives rise to an additional degree of freedom (pseudospin), which enables electrons to change the layer index.

Double layers may be categorized into two groups based on their physical properties: those with the Coulomb coupling and those with the tunnel coupling between the layers. Double layers with Coulomb couplings are of interest for fundamental research. Coulomb correlations between electrons of different wells may be responsible for physical phenomena such as Coulomb drag, ferromagnetism, superconductivity, and Wigner crystallization [29–32]. Double layers with tunnel bonds, in their turn, are interesting for technological applications. DQWs with a spatially modulated tunnel coupling are the most likely candidates for the creation of basic elements of quantum computers, qubits, and quantum logical gates integrated into standard electron circuits. By varying the number and distribution of surface gates for DQWs, it is possible to organize any quantum computation [33].

The additional degree of freedom gives rise to new oscillation branches, one of which resembles ion waves in gas plasma and others are analogous to exciton-type oscillations [34, 35]. In double-layer systems, Landau damping is also characterized by specific features. With the delay effects neglected, the dispersion equation for plasma waves in thin layers separated by a barrier d in the small-momentum region

$qa_B \ll 1$ has the form

$$\omega_{\mp}^2(q) = \frac{2\pi e^2 q}{\varepsilon m^*}(N_1 + N_2) \times \left[\frac{1}{2} \mp \frac{1}{2}\left(1 - \frac{4N_1N_2}{(N_1+N_2)^2}\left(1 - \exp(-2qd)\right)\right)^{1/2}\right], \quad (8)$$

where $N_{1,2}$ are the electron surface densities in each layer and a_B is the effective Bohr radius in a layer. In experimentally realized systems, $N_{1,2}$ are densities of ionized donors from two sides of a DQW and the phenomenological parameter d includes the nonlocality of electron wave functions in the direction of heterostructure growth. The distance between the centers of the DQW-forming quantum wells is a good approximation for d.

Equation (8) describes two branches of plasma oscillations. One is $\omega_+(q)$ (optic plasmon), corresponding to in-phase oscillations of particles in two wells and characterized by the root dispersion law usual for a two-dimensional plasmon. The other is $\omega_-(q)$ (acoustic plasmon), describing out-of-phase electron oscillations in DQWs with the acoustic dispersion [36, 37]. This branch is analogous to the ion sound in gas plasma in terms of the q-dependence and the decay mechanism. At $v_{F1} \neq v_{F2}$ (v_{Fi} is the Fermi velocity in the ith layer), one branch always (even at zero temperature) involves Landau damping: a plasmon in the layer with a lower Fermi velocity damps down on electrons of the other layer. At $qd \gg 1$, the layers become decoupled and Eqn (8) gives two independent 2D plasma waves. The plasmon phase velocity in either wave is higher than its 'own' Fermi velocity, that is, $\omega_1 > qv_{F1}$ and $\omega_2 > qv_{F2}$ for infinitely large q.

Double layers with tunnel couplings may contain three plasma branches. In symmetric DQW, one of them is an acoustic plasmon that damps down if the criterion

$$\left(\frac{1-n_2}{n_1}\right)\left[1 + \frac{a_B}{2D'(0)}\right]^2 < 1 \quad (9)$$

is not satisfied, where

$$D'(0) = \left.\frac{\mathrm{d}D}{\mathrm{d}k}\right|_{k=0}, \quad D(k) = I_{1111}I_{2222} - I_{1122}^2,$$

$$I_{ijkl} = \left\langle \psi_i(z)\,\psi_j(z)\right| \exp\left(-k|z-z'|\right) \left|\psi_k(z')\,\psi_l(z')\right\rangle,$$

$\psi_{1,2}(z)$ are the wave functions components along the growth axis in the symmetric and asymmetric dimensionally quantized subbands, and $n_{1,2}$ are electron surface densities in these subbands [34].

We note that the sum of surface densities in the subbands equals the sum of the densities of ionized donors in DQW barriers (the electroneutrality property), even though n_i and N_i taken separately are not equal. Criterion (9) usually fails to be satisfied, and the spectrum of two layers retains two plasma branches, in-phase and tunnel. The energy of the in-phase oscillations of the charge in the two subbands is not very sensitive to the tunnel coupling value and is determined by the total electron density. Properties of the second branch are considered below.

The dissipative conductivity of DQWs shows integer QHE states with an odd total filling factor in two layers. It is a rather surprising observation because single layers have no half-integer QHE states. It turns out that even weak interlayer tunneling gives rise to an odd-integer state of QHEs promoted by the opening of the energy gap between symmetric and antisymmetric subbands of dimensional quantization [38, 39]. The ground state is a single completely filled Landau spin sublayer of the symmetric subband separated from the corresponding Landau spin sublayer of the asymmetric subband by an energy gap. If the interlayer Coulomb interaction is sufficiently strong and the total filling factor is unity, the collective QHE state can be observed even in the absence of tunneling [40, 41].

At a certain critical distance between the layers, a phase transition occurs from the incompressible to the compressible QHE state, which is a superfluid quantum liquid, a boson condensate formed by electrons and holes in different layers [30, 42, 43]. The order parameter in the compressible state is introduced by analogy with superconductors or superfluid He^4 and its spatial fluctuations lead to the Goldstone mode. It is expected that the new state may be associated with the Kosterlitz – Thouless transition and with the Josephson and Meissner effects [44, 45]. Despite voluminous theoretical literature on double electron layers, experimental studies have largely been confined to magnetotransport investigations of the ground state. This is because the excitation of asymmetric modes during electromagnetic field absorption and emission is forbidden by symmetry, and the study of symmetric modes is of low informative value.

The objective of the present review is to discuss the results of experimental studies on excitations in single and double quantum wells that are inactive in the processes of absorption and emission of electromagnetic radiation. The review is organized as follows. Section 2 contains the description of an original experimental method for the measurement of inelastic light scattering spectra in perpendicular and tilted magnetic fields. Section 3 is focused on cyclotron excitations of spin density in single quantum wells, whose energy is sufficient to measure exchange and correlation interactions in integer-valued and fractional QHEs. Section 4 considers intersubband magnetoexcitation spectra in the small-momentum region, new branches of collective excitations, and experimental confirmation of a fundamental relation for the energy of the intersubband Bernstein modes in a spatially homogeneous system. Also discussed in this section are interactions of the intersubband Bernstein modes with the principal charge and spin density excitations and with excitations of the phonon subsystem of semiconductor quantum wells. Section 5 considers excitations and magnetoexcitations in double quantum wells and the effects of spatial asymmetry on collective excitations. It also describes a method for measuring asymmetry from the spectrum of single-particle excitations in a parallel magnetic field.

2. Experimental method

The authors have developed a method for the measurement of 2D electron system spectra in an arbitrarily oriented external magnetic field at superlow temperatures using a pair of optical waveguides. One lightguide serves to induce optical excitation of the electron system and the other to detect the inelastic light scattering signal. The detector lightguide is an effective in-situ premonochromator that filters laser radiation reflected from the sample surface and the entire signal of intrinsic inelastic light scattering from the exciting waveguide.

Because 2D systems have translational symmetry only in the quantum-well plane, inelastic light scattering processes retain the longitudinal component of a radiation pulse. This

opens up a unique possibility to study the dispersion of 2D excitations without readjustment of the exciting radiation wavelength. The pulse strength depends on the waveguide orientation with respect to the test sample surface and its maximum value is limited by the wavelength of the exciting photon. Both the waveguides and the test sample are firmly fixed on a rotating holder, with the sample attached at an arbitrary angle to the holder axis. The holder is placed in a cryostat with a superconducting solenoid in which the field is directed either horizontally or vertically. By rotating the holder in the solenoid with the horizontal field, it is possible to continuously vary the angle between the directions of the magnetic field, the pulse, and the normal to the 2D system. The horizontally oriented field is used to carry out experiments in the Foigt geometry, and the vertical orientation of the field allows experimenting with the Faraday geometry.

The waveguide technique for the study of inelastic light scattering has the advantage of being free from drawbacks inherent in the standard method using an optical window, such as contamination of the optical guide or misalignment of the optical system caused by magnetic field scanning. This technique enables measurements in parallel and perpendicular configurations of the polarization vectors of exciting and scattered photons [46]. Light polarization is analyzed by linear polarizers and phase-rotating plates placed in liquid helium straight in front of the test sample.

The present study was carried out using a group of high-quality heterostructures grown by molecular beam epitaxy. The heterostructures were asymmetric selectively alloyed $Al_xGa_{1-x}As/GaAs$ $(x = 0.3-1)$ 12–45-nm-wide single quantum wells and symmetric 12–25-nm-wide double quantum wells separated by insulating barriers 2.5–5 nm in width. The electron densities were $(1-7) \times 10^{11}$ cm^{-2} and mobilities of the order $(1-10) \times 10^6$ cm$^{2\,-1}$ s^{-1}. The density of the heterostructures was varied as described in [47]. The same method was used to balance double quantum wells.

3. Combined cyclotron excitations in single quantum wells

This section deals with investigations into inelastic light scattering by combined electron excitations associated with concomitant variations in the Landau level number and spin quantum number. Combined excitations are essentially different from excitations actively absorbing electromagnetic radiation, i.e., magnetoplasmons and magnons. The energy of the latter satisfies the Kohn and Larmor theorems. The Kohn theorem forbids contributions to the magnetoplasmon energy from the electron–electron interaction in a spatially homogeneous system and the Larmor theorem forbids contributions to the magnon energy in a system invariant under rotations in the spin space. No such limitations are imposed on the energy of combined excitations, and their experimental observation opens up a unique possibility to study electron–electron interactions in 2D systems.

Section 3.1 is focused on combined excitations in the ultraquantum limit when the electron filling factor at the lowest Landau level is smaller than 1/2 [48]. A new quantum excitation, a cyclotron spin wave in the range of filling factors from 1 to 2 [49], is discussed in Section 3.2. Section 3.3 is devoted to considering a special case of even integer filling factors [50].

3.1 Combined cyclotron excitations in the ultraquantum limit

It is convenient to start the description of the properties of combined excitations from the ultraquantum limit $\nu \sim 1/10$ in which Coulomb correlations play only an insignificant role. Almost all electrons in the ultraquantum limit are bound to positively charged impurities, thus giving rise to complexes located in the AlGaAs barrier of the quantum well [52]. In the range of magnetic fields under consideration, the lowest energy is inherent in the singlet state of a localized trion, a three-particle complex in which two electrons with different spins in the quantum well are bound to a charged impurity in the barrier [51]. This accounts for the zero spin quantum number of the ground state and the division of excitations into singlet or triplet.

The inelastic light scattering spectrum consists of four lines, two of which coincide and have the energy equal to the cyclotron energy, whereas the energy difference between two others is as large as the Zeeman energy. The coincident lines correspond to the magnetoplasmon ($m = 1$, $S = 0$, $S_z = 0$) and spin wave ($m = 1$, $S = 1$, $S_z = 0$), respectively, while the split ones correspond to spin-flip modes ($m = 1$, $S = 1$, $S_z = \pm 1$) (Fig. 1). As the filling factor grows, the exchange interaction between electrons at the zero Landau level leads to a rise in the effective g-factor of the electrons. As a

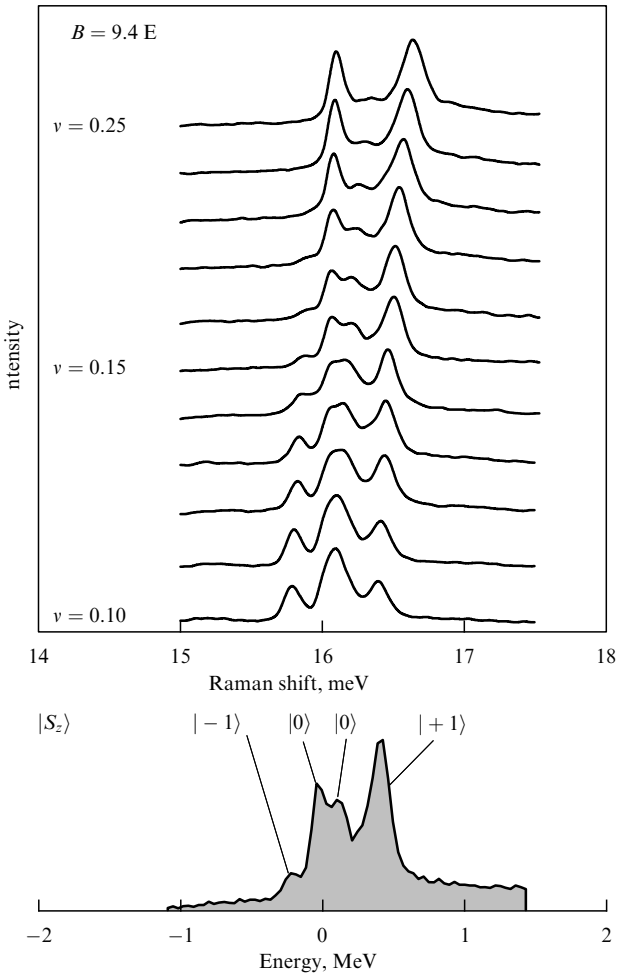

Figure 1. Inealstic light scattering spectra of a quantum well in the cyclotron energy region at different filling factors. The bottom figure presents classification of spectral lines and their energy counted from the cyclotron energy.

consequence, the electron system acquires spin polarization, which results in the disappearance of the spin wave line and a low-energy spin-flip mode. The energy of the second spin-flip mode simultaneously increases. The energy difference between the high-energy spin-flip mode and the magnetoplasmon is reflected in the amount of the exchange-correlation energy that is lost by the electron during transition from the zeroth to the first Landau level.

Comparison between theory and experiment reveals a two-fold exceeding of the computed value over the observed one if only exchange interaction is taken into account. Such a substantial discrepancy between theoretical and experimental findings ensues from the correlation between electrons at a partially filled Landau level. This inference can be verified in the framework of the single-mode approximation proposed by Feynman for the description of phonons in superfluid helium [53]. Excitation energies are given by

$$E(\mathbf{k}) = \frac{F(\mathbf{k})}{S(\mathbf{k})} ,$$

where

$$S(k) = \int \mathrm{d}\mathbf{r} \, \exp(-\mathrm{i}\mathbf{k}\mathbf{r}) \left[g(\mathbf{r}) - 1\right]$$

is the static structural factor, $g(\mathbf{r})$ is the pair correlation function, and $F(\mathbf{k})$ is the oscillator strength [54]. When the filling factor has an arbitrary value, the correlation function remains unknown, but its numerical approximation for certain Laughlin states of fractional QHEs can be obtained by the Monte Carlo method [14, 55]. Taking correlations in both the ground and excited states into account significantly reduces the energy of the spin-flip mode, in excellent agreement with experiment (Fig. 2) [48, 56].

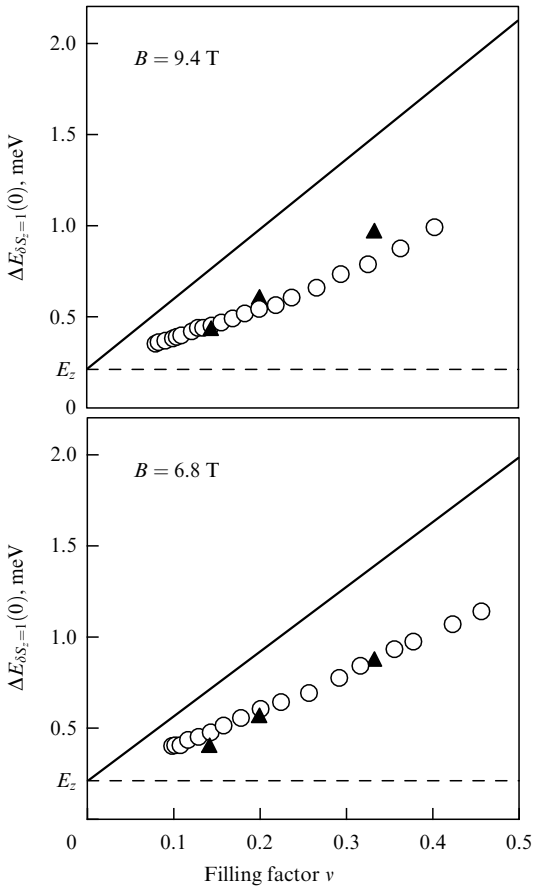

Figure 2. Experimentally found difference between the spin-flip mode and magnetoplasmon energies for two magnetic field values depending on the electron filling factor ν (circles); triangles and solid lines represent values calculated in the framework of the single-mode and Hartree – Fock approximations, respectively; dashed lines show the Zeeman energy E_z.

We note that the spin-flip mode, unlike the magnetoplasmon, is a decay excitation because an electron system may contain pairs of excited states with the same energy, total generalized momentum, and spin quantum number that consist of a spin exciton ($m = 0$, $\delta S = 1$, $\delta S_z = +1$) and a magnetoplasmon ($m = 1$, $\delta S = 0$, $\delta S_z = 0$).

Indeed, it is observed in experiment that the linewidth or the inverse lifetime of the spin-flip mode significantly increases as the filling factor changes from $\nu = 1/10$ to $\nu = 1/2$. Conversely, no line corresponding to the spin-flip mode can be detected at the filling factor $\nu = 1/2$ because its lifetime is very short [48]. In the range of $\nu \to 1$, the line of the spin-flip mode narrows again, probably due to a decrease in the number of decay channels in the integer QHE state. A further rise in the filling factor leads to spin depolarization of the electron system, whereas the lifetime of the spin-flip mode continues to decrease.

3.2 Cyclotron spin wave

The filling of the second spin Landau sublevel ($\nu > 1$) is accompanied by a new collective excitation of the charge-spin type or a cyclotron spin wave (Fig. 3). The magnetoplasmon and cyclotron spin wave represent in-phase and out-of-phase oscillations of the spin subsystem in a 2D electron system with the cyclotron frequency. In the case of a zero generalized momentum, the cyclotron spin wave is a spin-type excitation, whereas in the shortwave limit $ql_B \to \infty$, it becomes a charge-type excitation [57].

In the longwave limit, the cyclotron spin wave is dispersionless and its energy equals the cyclotron energy and is independent of the electron distribution over two spin Landau sublevels. Therefore, the spin wave energy may be regarded as a measure of the cyclotron electron mass more accurate than the cyclotron resonance energy. It is known that longwave fluctuations of a random potential from the ionized donor level in 2D systems cause a shift of the cyclotron resonance energy toward the energy of a magnetoplasmon with the momentum given by the inverse length of fluctuations, while the energies themselves differ in samples with different distributions of the impurity potential [58]. The energy of the cyclotron spin wave is resistant to fluctuations of the random potential, and the tilt of its magnetic field dependence may be used to accurately determine the cyclotron mass of electrons [49].

3.3 Spin-triplet excitations in even integer QHE states

A special case for combined cyclotron excitations is the filling factor $\nu = 2$, at which the ground state of a 2D electron system is not spin-polarized ($S = 0$) and the excited states may be classified as singlet or triplet. It is assumed that the state $\nu \to 2$ is equivalent to the state $\nu \to 0$ considered above because the properties of an electron system at a virtually vacant Landau level are equivalent to the properties of a hole system at an almost completely filled Landau level (the electron – hole symmetry). The energies of excitations at $q = 0$ in the first order of smallness in the parameter $r_c = (e^2/\varepsilon l_B)/\omega_c$ coincide at $\nu = 2$ and $\nu \to 0$.

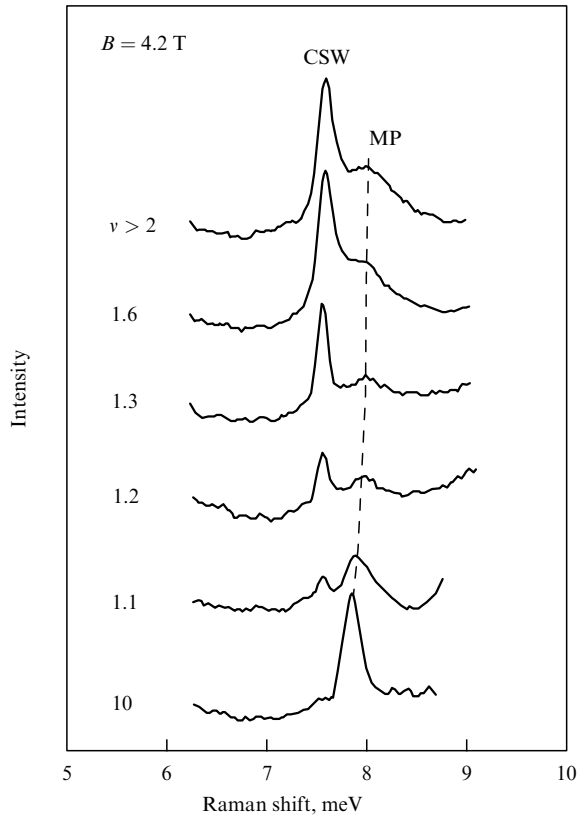

Figure 3. Inelastic light scattering spectra at $B = 4.2$ T and different electron filling factors. In an electron system with a single filled spin Landau sublevel, there is only an in-phase cyclotron excitation, the magnetoplasmon (MP). Filling of the second spin sublevel $\nu > 1$ opens up the possibility for the formation of an out-of-phase excitation, the cyclotron spin wave (CSW).

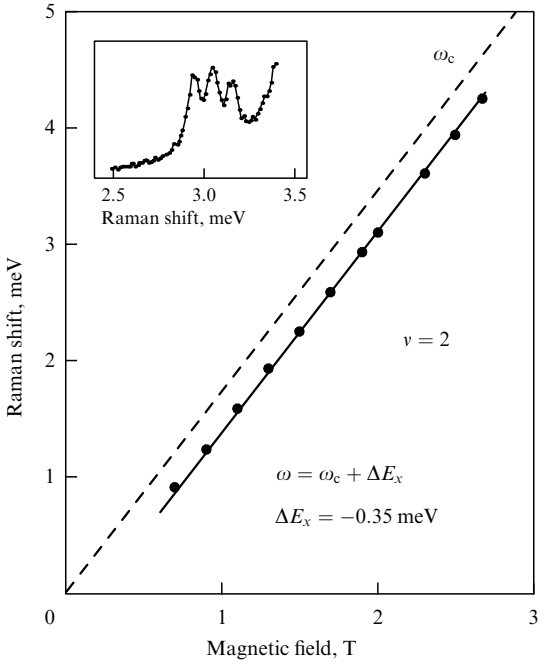

Figure 4. Magnetic field dependence of the energy of a spin-triplet magnetoexciton at the electron filling factor $\nu = 2$. The dashed line represents the cyclotron energy. The inset shows the characteristic spectrum of inelastic light scattering.

It can be shown that Coulomb corrections to the energy of spin-triplet excitations also vanish in the remaining orders of the perturbation theory. However, exchange corrections to the spin-triplet excitation energy do not vanish even in the second order. Exchange interaction decreases the energy of spin-triplet excitations relative to the cyclotron resonance energy, while the exchange contribution ΔE_x is independent of the magnetic field (Fig. 4). Such a behavior of the exchange energy leads to a nontrivial physical result. The energy needed to transfer an electron to the first Landau level from the zeroth level and simultaneously invert its spin is lower than the cyclotron energy. Because second-order corrections 'work' in relatively small fields, the exchange contribution makes a considerable portion of the cyclotron energy, while the Zeeman energy may be infinitely low.

Summation of all exchange corrections in the second order of the perturbation theory gives the exchange contribution value

$$\Delta E_x = -\sum_{n=2}^{\infty} R_n \frac{1 - 2^{1-n}}{n(n^2-1)}, \qquad (10)$$

where

$$R_n = \frac{2}{n!}\int_0^{\infty} \mathrm{d}q\, q^{2n+3} V^2(q) \exp(-q^2)$$

in units of $r_c^2\omega_c \approx 11.34$ meV. In an ideal 2D system, $\Delta E_x = (\ln 2 - 1)/2 = -0.1534\ldots$ [50, 59]. In a real 2D electron system, the nonlocality of electron wave functions in the direction of a quantum well smoothes the Coulomb interaction. Then, the 2D expression for $V(q) = 1/q$ should be substituted by $V(q) = F(q)/q$, where $F(q)$ is the formfactor depending on the quantum well width and electron density. With the formfactor taken into account, the exchange contribution value is in good agreement with experimental data.

We note that exchange contributions of the second order reduce the energy of spin-triplet excitations not only at $\nu = 2$ but also in all other integer QHE states. The exchange contribution simultaneously decreases due to the 'broadening' of magnetoexciton wave functions. By way of example, the negative exchange contribution to the energy of a spin-triplet magnetoexciton at $\nu = 4$ is two times smaller than that at $\nu = 2$ [50].

4. Intersubband magnetoexcitations in single quantum wells

This section is concerned with the modification of intersubband excitations by a magnetic field. Similarly to combined cyclotron excitations, the majority of intersubband excitations are not active in absorbing electromagnetic radiation; hence, inelastic light scattering is the sole method suitable for their investigation. Section 4.1 presents experimental verification of a Kohn theorem analog for intersubband excitations and examines new branches of intersubband magnetoexcitations related to the multicomponent nature of the ground state of the electron system with a few filled Landau levels [60, 61]. Section 4.2 discusses dispersion dependences of intersubband excitations and information on the collective properties of 2D electron systems, the interaction between collective

modes of different natures, and the interaction of the electron and phonon subsystems of quantum wells [60, 62, 63]. Finally, Section 4.3 is devoted to the effect of a parallel magnetic field on the energy of intersubband excitations and magnetoexcitations [64].

4.1 Intersubband magnetoexcitations with zero generalized momentum

We first consider the well-known spectrum of intersubband excitations in a zero field. It comprises two collective modes of the exciton type that may be regarded as singlet and triplet states of the exciton formed by an electron in the excited subband and a hole below the Fermi level of electrons in the ground subband [65–68]. At $q \to 0$, the energy of the triplet exciton is smaller than the single-particle energy of intersubband splitting due to the Coulomb interaction between the electron and the hole (the exciton shift). The energy of a singlet exciton may be either higher or lower than the single-particle energy. Besides the exciton shift, it contains the energy of the macroscopic polarization electron system (the depolarization shift).

Inelastic light scattering shows two narrow lines of exciton-like collective excitations and a broad line corresponding to the continuum of single-particle excitations (Fig. 5) [66]. In a magnetic field perpendicular to the quantum well plane, the continuum of single-particle excitations splits into a number of individual spectral components corresponding to the intersubband Bernstein modes, i.e., collective excitations occurring with simultaneous changes of the Landau level number and of the index of the dimensionally quantized subband change. The energies of the intersubband Bernstein mode give rise to a 'fan' of Landau levels stemming from the energy of intersubband splitting with the slope determined by the effective electron mass in a semiconductor quantum well:

$$E_{\mathrm{B}\pm n} = |\Omega \pm n\omega_{\mathrm{c}}| \,, \tag{11}$$

where $|n| \geqslant 1$ and Ω is the single-particle energy of intersubband splitting.

Fundamental expression (11) is an analog of the Kohn theorem for intersubband excitations: *the energies of intersubband Bernstein modes at a zero momentum do not depend on the electron–electron interaction* [60, 69–71]. It is noteworthy that expression (11) contains no contributions reflecting peculiarities of the confining potential of the quantum well (shape, width, and height), and the single-particle energy Ω is the sole parameter that characterizes the transverse motion of electrons.

Unlike in the case of Bernstein modes, the energies of singlet and triplet excitons are independent of the magnetic field. These excitations are transformed into magnetoexcitons related to electron transitions with the conserved Landau-level number. In neglecting the nonparabolicity of the conductivity band in the energy range of intersubband splitting, the energies of all such transitions are equal to each other and show no dependence on the magnetic field value.

When more than one Landau level is filled in the ground state of a 2D electron system, additional excitation branches emerge in which the number of a given Landau level remains unaltered. These are out-of-phase electron oscillations from different Landau levels. They are presented in an inelastic light scattering spectrum by the L_0 resonance [60, 61]. When n

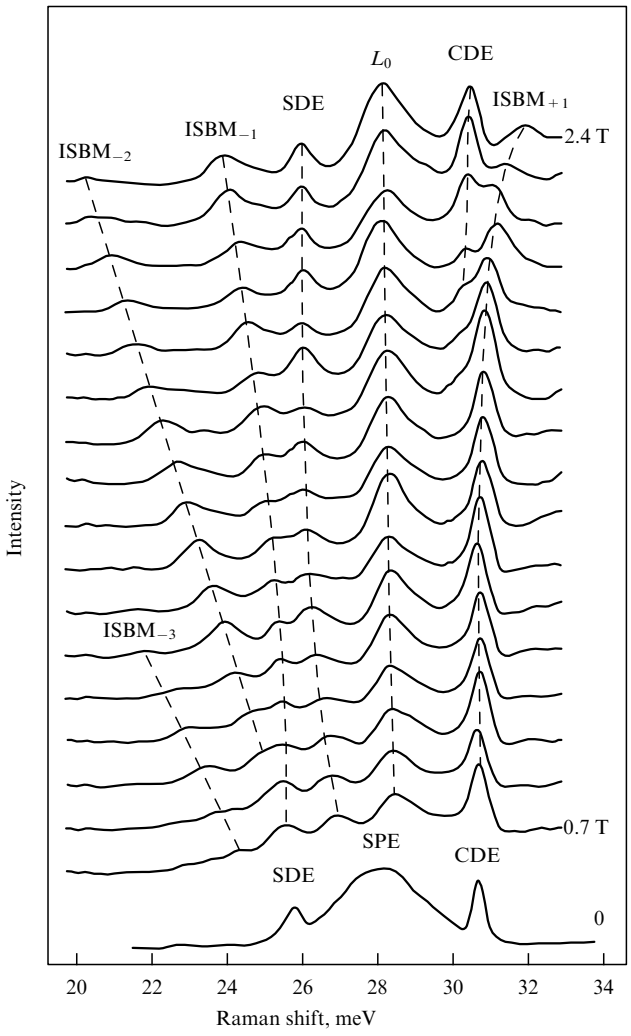

Figure 5. Inelastic light scattering spectra of intersubband excitations with an interval of 0.1 T in the range from 0.7 to 2.4 T at $q = 0.4 \times 10^5$ cm^{-1}. The spectrum in a zero magnetic field is presented for comparison. Notation: SPE — single-particle continuum, ISBM — intersubband Bernstein modes, CDE and SDE — spin-singlet and spin-triplet intersubband excitons, L_0 — out-of-phase modes.

Landau levels are filled in the ground state, there are $2n$ collective intersubband branches joined in pairs, each comprising charge and spin density excitations. The energies of one pair are independent of the magnetic field; they are in-phase branches (singlet and triplet intersubband magnetoexcitons). The energies of all the remaining (out-of-phase) branches decrease as the magnetic field increases; as $B \to 0$, they converge to the energy of single-particle intersubband splitting. Splitting of the in-phase branches is as large as the depolarization shift. The energies of the out-of-phase branches coincide within each pair and their interpair difference is small [72, 73].

In a sense, the above branches are analogous to phonons in crystals. An elementary crystal cell corresponds to a magnetic flux quantum in an electron system. In-phase intersubband branches are analogous to the acoustic branch. Their energies are determined by the total electron density in a 2D system. All other out-of-phase branches are analogous to optical branches. Their number for each excitation type (charge or spin density) is $n - 1$; these branches are absent at $\nu < 2$, when there is only one electron

of each spin per magnetic flux quantum [61]. Naturally, the analogy between phonons and collective magnetoexcitations is provisional. For example, the electron filling factor is a continuous function of the magnetic field, whereas the number of atoms in an elementary cell changes discretely. As a result, the energies of out-of-phase branches vary monotonically with alteration of the filling factor.

4.2 Dispersion of intersubband magnetoexcitations in the longwave limit

Relation (11) describes the behavior of the intersubband Bernstein modes at $ql_B \to 0$. As the momentum grows, their energies deviate from the linear dependences in the energy resonance region with intersubband magnetoexcitons. Coulomb interactions result in hybrid collective excitations with and without altering the numbers of the Landau levels; the hybrid gaps are proportional to $(ql_B)^{|n|}$, where n is the Bernstein mode number [60]. The size of the hybrid gaps and the character of their dispersion dependences are consistent with theoretical predictions in the framework of the local density approximation (Fig. 6) [65, 69, 74, 75].

The dependences of hybrid gaps on the electron density exhibit some interesting features. The upper hybrid gaps $n \geqslant 1$ disappear at a certain critical (nonzero) electron density found from the condition of equality of the depolarization and exciton shifts (Fig. 7). At densities below the critical value, the energy of a singlet intersubband exciton becomes smaller than the energy of single-particle intersubband splitting, and the energy resonance with the Bernstein modes is unfeasible.

The upper hybrid gaps exhibit a nonmonotonic dependence on the electron density by virtue of the dynamic screening of the Coulomb interaction by optical phonons. As a result of band bending in the semiconductor quantum well, a rise in the electron density inevitably leads to an enhanced energy of intersubband splitting. Simultaneously, the energy of the singlet intersubband exciton increases and, at a certain electron density, comes into resonance with a longitudinal optic phonon. The macroscopic polarization field merges the electron and phonon modes, and the inelastic light scattering spectrum exhibits two hybrid modes [62].

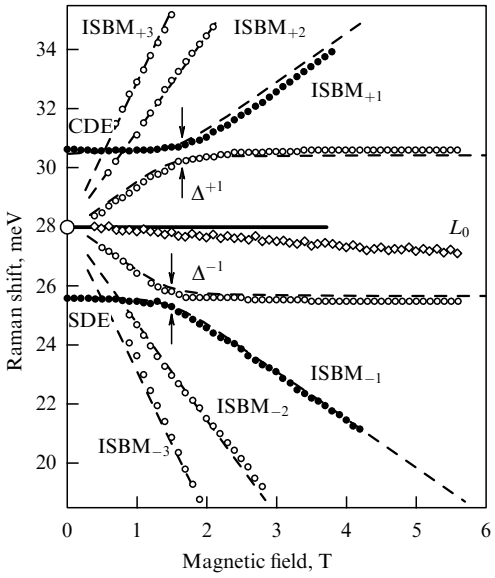

Figure 6. Energies of intersubband excitations: dots — experiment, dashed lines — values calculated in the local density approximation. The maximum of the single-particle continuum is represented by the white circle.

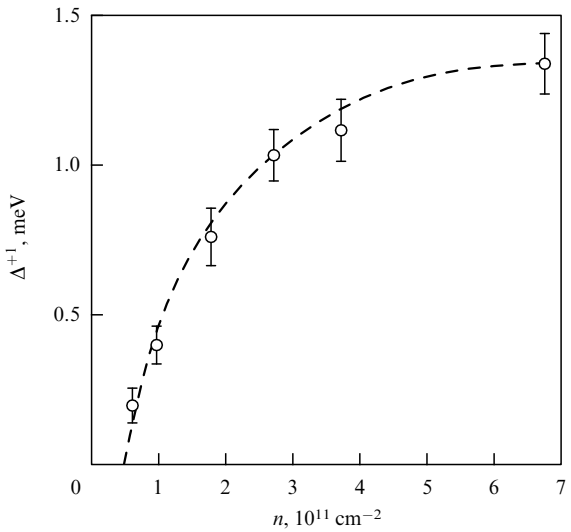

Figure 7. The plot of hybrid gap Δ^{+1} versus electron density at a fixed value of momentum $q = 1.1 \times 10^5$ cm^{-1}; the dashed line represents the results of calculations in the local density approximation.

The hybrid modes in their turn interact with the intersubband Bernstein modes, giving rise to triple modes (Fig. 8). The Bernstein modes themselves do not interact with the optical phonon mode, at least in the longwave limit; instead, they interact only with the electron component of hybrid modes. The interaction of the Bernstein modes with the electron component of the hybrid mode is enhanced and the interaction with the phonon mode impaired if the parameters of quantum wells are changed such that the singlet exciton is out of resonance with the optical phonon.

4.3 Intersubband excitations and magnetoexcitations in a parallel magnetic field

Intersubband excitations in parallel and tilted magnetic fields show unusual properties. Nonlocality of the electron wave functions in the direction of the quantum well growth makes electrons and holes of intersubband excitations propagate in two spatially separated planes. They are dipoles with the dipole moments

$$\mathbf{d} = -e \mid z_{00} - z_{11} \mid \mathbf{n}\,, \tag{12}$$

where $\mathbf{n}$ is the normal to the well plane,

$$z_{00} - z_{11} = \int \mathrm{d}z\, \psi_0^*(z)\, z\, \psi_0(z) - \int \mathrm{d}z\, \psi_1^*(z)\, z\, \psi_1(z)$$

is the mean distance between the electron and the hole, and $\psi_i(z)$ is the component of the electron wave function in the direction of the quantum well growth in a dimensionally quantized subband with index i.

In the external magnetic field oriented along the well plane, the vector

$$\mathbf{P} = \mathbf{\Pi} + \frac{1}{c}\,\mathbf{d} \times \mathbf{B} \tag{13}$$

plays the role of the generalized momentum of intersubband excitations conserved in scattering processes ($\mathbf{P} = \mathbf{q}$), where $\mathbf{\Pi}$ is the kinematic momentum in the well plane [76].

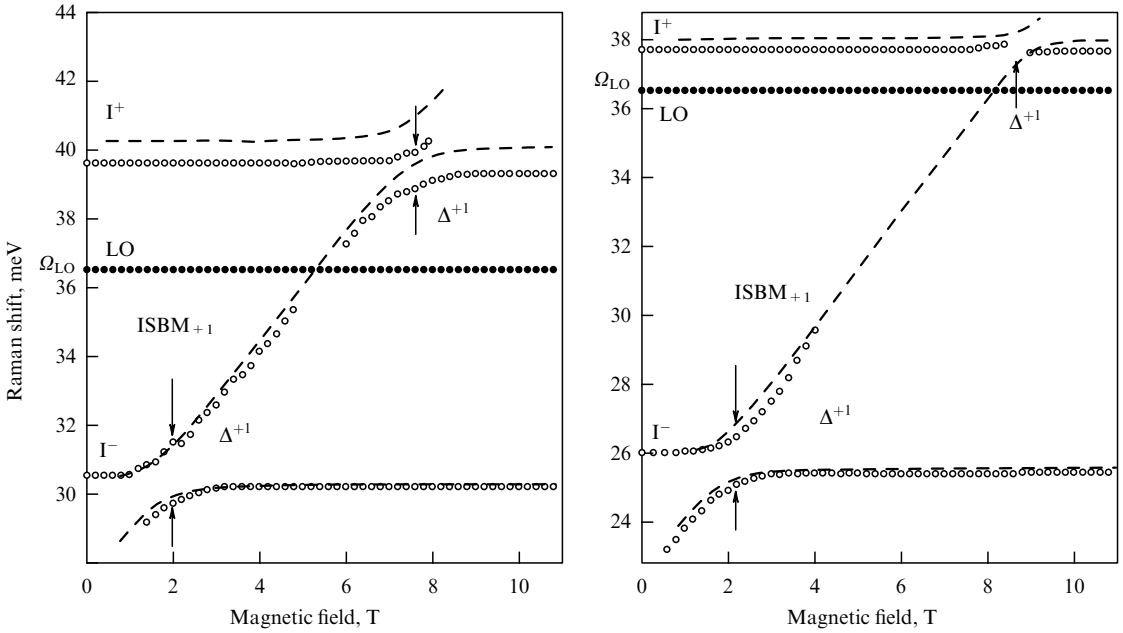

Figure 8. Energies of intersubband magnetoexcitations in the LO-phonon frequency range at two values of the intersubband splitting energy; white circles: experiment, dashed lines: theory. Hybrid electron – phonon modes are denoted as I^+ and I^-. The energy of the bulk LO-phonon represents the reference level (black dots).

The kinetic energy of intersubband excitations is a function of the kinematic momentum

$$E(\mathbf{\Pi}) = E\left(\left|\mathbf{P} - \frac{1}{c}\,\mathbf{d}\times\mathbf{B}\right|\right), \tag{14}$$

which means that the energy involves the gauge term $c^{-1}\mathbf{d}\times\mathbf{B}$, in addition to the generalized momentum. This allows studying the dispersion of intersubband excitations by applying an in-phase magnetic field. The condition

$$\mathbf{P} = \frac{1}{c}\,\mathbf{d}\times\mathbf{B} \tag{15}$$

being satisfied, the kinematic momentum and, accordingly, the kinetic energy vanish, although neither the generalized momentum nor the gauge term taken separately are equal to zero.

The influence of the gauge term on intersubband excitation energies is illustrated using a singlet intersubband exciton as an example (Fig. 9). When the momentum is zero, its energy depends on the magnetic field quadratically. As the longitudinal momentum along the vector $\mathbf{d}\times\mathbf{B}$ grows, the magnetic field dependence shifts on the abscissa axis by the value of the momentum. This means that the magnetic field dependence of the excitation energy may be identified with the dispersion dependence.

When the relative orientation of $\mathbf{q}$ and $\mathbf{d}\times\mathbf{B}$ changes without alteration of their absolute values, the kinetic energy shows rotational anisotropy (Fig. 10), while its angular dependence is fairly accurately described by expression (14):

$$E(\mathbf{\Pi}) = \frac{1}{2m^*}\left(\mathbf{q} - \frac{1}{c}\,\mathbf{d}\times\mathbf{B}\right)^2, \tag{16}$$

where m^* is the effective mass of the singlet intersubband exciton. Although individual intersubband excitations are characterized by different quantum numbers of the internal and spin degrees of freedom, they have equal dipole moments and their dispersion dependences behave similarly [64].

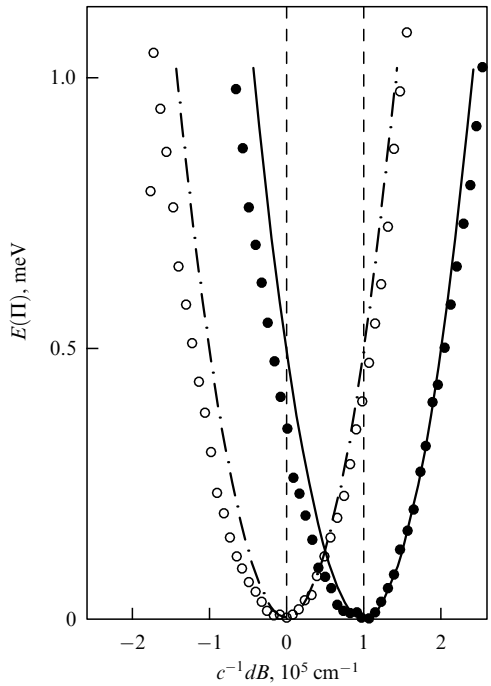

Figure 9. Experimental dependence of the kinetic energy of a singlet intersubband exciton on $c^{-1}dB$ for two values of the inelastic light scattering momentum: $q = 0$ (white circles) and $q = 1\times10^5$ cm^{-1} (black circles). The vector $\mathbf{d}\times\mathbf{B}$ is directed along $\mathbf{q}$. Dash-dotted lines represent singlet exciton dispersion values calculated in the framework of the local density approximation; solid line is the same dispersion curve displaced by 1×10^5 cm^{-1} along the abscissa axis.

A special case is constituted by single-particle excitations that are not bound complexes characterized by an intrinsic dispersion dependence. The energies of single-particle and collective excitations show different dependences on the

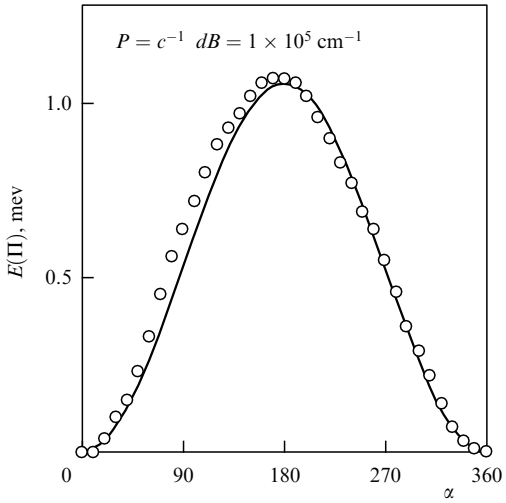

Figure 10. Experimentally found dependence of the kinetic energy of a singlet intersubband exciton on the angle α between the directions of the vectors $\mathbf{q}$ and $\mathbf{d} \times \mathbf{B}$ at $q = c^{-1}dB = 1 \times 10^5$ cm^{-1} (circles). The solid line represents the calculated dependence $E(\Pi) = (1/2m^*)(\mathbf{q} - c^{-1}\,\mathbf{d} \times \mathbf{B})^2$.

angle between the generalized momentum and the magnetic field. In fact, the parallel field provides a powerful experimental tool for differentiating between collective and single-particle excitations, a serious experimental problem in the physics of excitations of low-dimensional systems. Relations (14) and (15) are also useful for finding a quantitative measure of the asymmetry of the quantum well confining potential, i.e., the dipole moment of intersubband excitations. The knowledge of the dipole moment allows determining the direction and the magnitude of the potential gradient. Moreover, the anisotropic part of the excitation energy being a linear function of the magnetic field, the measurements are feasible in small magnetic fields.

We consider the dispersion of intersubband excitations in an external magnetic field oriented at an arbitrary angle to the quantum well plane (Fig. 11). In this case, the kinematic momentum in expression (14) should be substituted by generalized momentum (4). Then, the parallel field effect on the excitation energy is again reduced to the gauge term $c^{-1}\,\mathbf{d} \times \mathbf{B}$. This can be shown in the example of the dispersion dependence of hybrid modes in the region of the resonance between a singlet exciton and an intersubband Bernstein mode with index +1. When the magnetic field is oriented orthogonally to the quantum well plane, the dispersion of the hybrid gap or the total dispersion of two hybrid modes becomes linear. The same dependence exists if the generalized momentum is fixed and the magnetic field component is varied such that the vectors $\mathbf{q}$ and $\mathbf{d} \times \mathbf{B}$ are codirected and the dependence is shifted along the axis of abscissas by the value of the generalized momentum (Fig. 12). The hybrid gap is nonexistent when $\mathbf{q} = c^{-1}\,\mathbf{d} \times \mathbf{B}$, although neither the generalized momentum $\mathbf{q}$ nor $c^{-1}\mathbf{d} \times \mathbf{B}$ taken separately is equal to zero. It may be concluded that the form of the dispersion dependence of intersubband excitations in the case of an arbitrary orientation of the magnetic field is determined by the perpendicular component of the field alone. Its parallel component displaces the dispersion dependence in the momentum space by the value of the gauge term. Using a parallel magnetic field, it is possible to measure the dispersion of intersubband magnetoexcitations in the region of

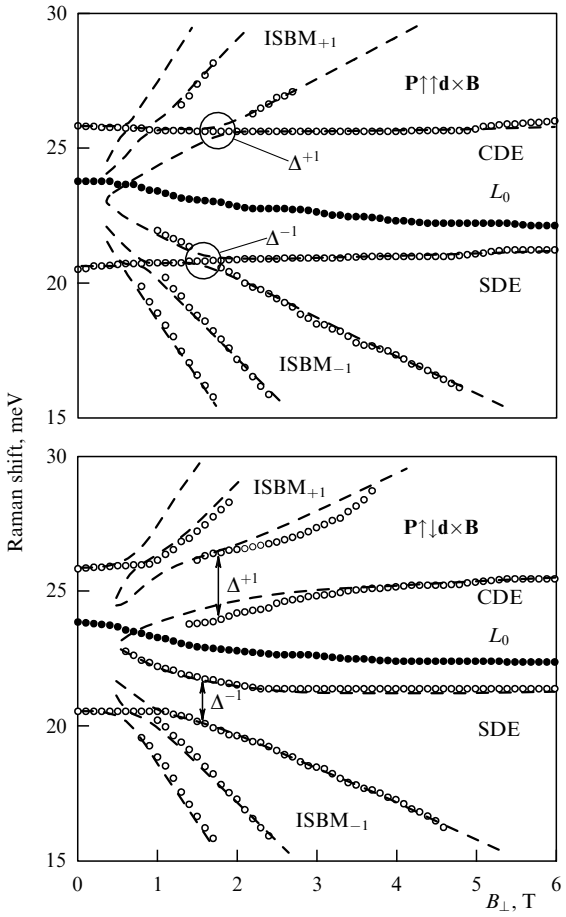

Figure 11. Inelastic light scattering spectra at $q = c^{-1}dB$ when the vectors $\mathbf{d}$ and $\mathbf{d} \times \mathbf{B}$ are codirected (top) and oppositely directed (bottom). Dashed lines represent theoretical excitation energies calculated in the local density approximation on the assumption that the parallel component of the magnetic field contributes to the excitation energy only through the gauge term $c^{-1}\mathbf{d} \times \mathbf{B}$, i.e., $P = 0$ (top) and $P = 2 \times 10^5$ cm^{-1} (bottom).

momenta unattainable in standard inelastic light scattering experiments [64].

5. Excitations and magnetoexcitations in double quantum wells

Intersubband excitations in single quantum wells have much in common with intersubband (interlayer) excitations in double quantum wells. It was accepted in the past that the principal physical parameter characterizing properties of the ground and excited states in DQW is the ratio of the tunnel energy Δ_{SAS} to the Fermi electron energy E_{F}. It is demonstrated in the present section that the degree of spatial asymmetry is a more important characteristic. This inference ensues from the fact that the ratio of the tunnel energy to the Fermi energy cannot be made arbitrarily small while preserving the symmetry of a given electron system. At a certain value of this ratio, the ground state symmetry is broken and the transition parameter is determined not only by the tunnel and Fermi energies but also by the well widths and the random impurity potential distribution.

Below, we call a state symmetric or asymmetric depending on whether the wave functions of single-particle states have or do not have parity. Documentation of the degree of DQW asymmetry is a very important experimental problem, dis-

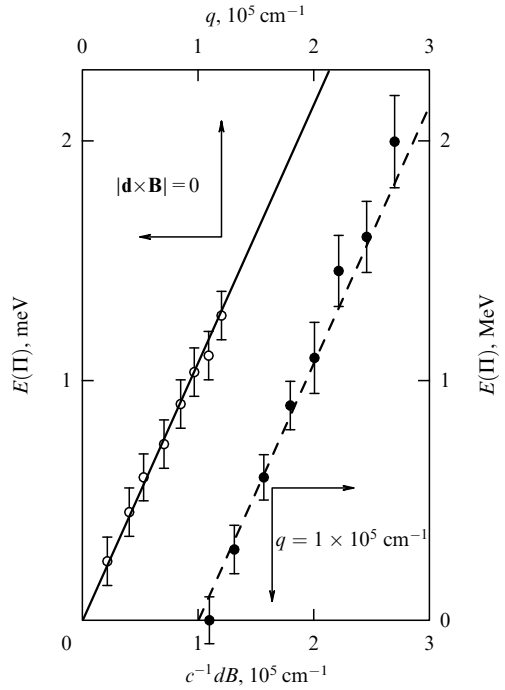

Figure 12. The energy of a singlet intersubband exciton at $B_\perp = 1.5$ T as a function of the generalized momentum at $c^{-1}dB = 0$ and of the vector $c^{-1}\mathbf{d}\times\mathbf{B}$ codirected with the vector $\mathbf{q}$ at $q = 1\times10^5$ cm^{-1}; the solid line is the linear approximation of experimental points, the dashed line is the same approximation shifted by 1×10^5 cm^{-1}.

cussed in Section 5.1 [77, 78]. The effects of asymmetry on plasma excitations are considered in Section 5.2 and on magnetoexcitations in Section 5.3 [79 – 81].

5.1 Single-particle excitations in double quantum wells in a parallel magnetic field

In what follows, we consider the spectrum of intersubband single-particle excitations in asymmetric DQWs. In the weak-tunneling limit $\Delta_{SAS} \ll E_F$, wave functions of single-particle states are localized in separate layers. For each value of the momentum, there is a continuum of single-particle excitations from under the Fermi surface of electrons of the first dimensionally quantized subband to the empty states over the Fermi surface of the second subband. In asymmetric DQWs, such excitations occur between different layers.

The boundary energies of the continuum, $\Omega - qv_F$ and $\Omega + qv_F$, are achieved for the excitations whose momentum is either parallel or antiparallel to the Fermi momentum of electrons in the first subband. As the momentum grows, the energies change in opposite directions. The phase space of the second subband being filled, the density of states for resonances between inelastic light scattering and boundary energies is considerably higher than for the remaining part of the continuum; therefore, the spectrum consists of two lines with boundary energies of the continuum [77, 82]. Extrapolation of their energies to $q = 0$ yields the intersubband splitting Ω and the slope of linear dependences gives the Fermi velocity of electrons in the first dimensionally quantized subband.

According to (14), excitation energies at the boundaries of the continuum show a linear dependence on the magnetic field oriented along the DQW plane:

$$E = \Omega \pm qv_{F1} + \frac{1}{c}\, dBv_{F1}$$

if $\mathbf{q}$ and $\mathbf{B}$ are parallel, and

$$E = \Omega \pm \left|\mathbf{q} - \frac{1}{c}\,\mathbf{d}\times\mathbf{B}\right| v_{F1}$$

if $\mathbf{q}$ and $\mathbf{B}$ are perpendicular to each other. Here, $v_{F1(2)}$ is the Fermi velocity in the first (second) subband.

We consider changes in the excitation spectrum during the transition of a DQW from the asymmetric to the symmetric state, taking a nonrealistic model of virtual excitations between two isolated quantum wells as an example (Fig. 13).

Excitation energies decrease proportionally to a fall in the energy of intersubband splitting, while the critical magnetic field at which condition (15) is satisfied does not change because the dipole moment remains constant.

A nontrivial situation occurs when the term $\left|\mathbf{q} - c^{-1}\,\mathbf{d}\times\mathbf{B}\right| v_{F2}$ exceeds the intersubband splitting energy. In this case, the spectrum contains two branches of single-particle excitations corresponding to direct transitions of electrons from a high-density layer to one of lower density (A-branch):

$$\left[\Omega - \left|\mathbf{q} - \frac{1}{c}\,\mathbf{d}\times\mathbf{B}\right| v_{F1}\,,\ \Omega + \left|\mathbf{q} - \frac{1}{c}\,\mathbf{d}\times\mathbf{B}\right| v_{F1}\right],$$

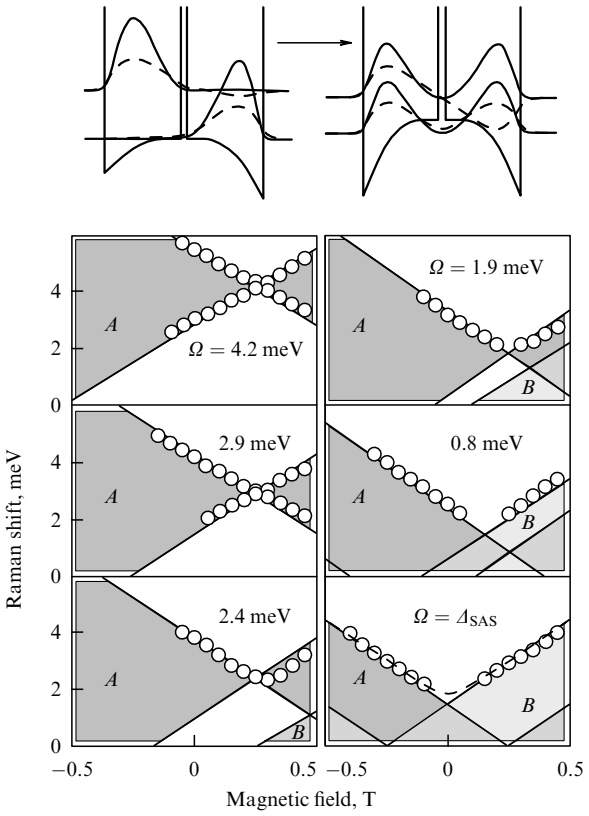

Figure 13. Variation of the DQW intersubband excitations spectrum during transition from the asymmetric to the symmetric state. The top figure depicts the limiting potential profile, wave functions (dashed lines), and squared wave functions (solid lines) in asymmetric (left) and symmetric (right) states. Shaded zones correspond to excitations from the first to the second quantum subband (A-branch), light ones to excitations from the second to the first subband (B-branch) disregarding tunneling. Zones where the energies of the two branches coincide are marked with light hatching and experimental points by white circles. The intersubband splitting energy for each state is denoted by Ω.

and to reverse transitions (B-branch):

$$\left[0, -\Omega + \left|\mathbf{q} - \frac{1}{c}\,\mathbf{d}\times\mathbf{B}\right| v_{F2}\right].$$

Excitations of either branch have dipole moments of equal moduli but opposite directions. Therefore, as the energy of one branch in a magnetic field increases, that of the other branch decreases. At certain values of system parameters,

$$\Omega < \frac{1}{2}\left(\left|\mathbf{q} - \frac{1}{c}\,\mathbf{d}\times\mathbf{B}\right| v_{F2} - \left|\mathbf{q} - \frac{1}{c}\,\mathbf{d}\times\mathbf{B}\right| v_{F1}\right),$$

the upper boundary of the B-branch exceeds that of the A-branch, which leads to symmetrization of the excitation spectrum (Fig. 13).

This model describes virtual interlayer excitations having the same dipole moment in any state. In real DQWs, symmetrization leads to a decrease in the dipole moment of excitations. Nevertheless, excitation energies in a symmetric state undergo a shift in a magnetic field as if the dipole moment of excitations were retained, because, in contrast to the case of single quantum wells, the splitting between symmetric and asymmetric subbands in DQWs is smaller than or comparable to the magnetic quantization energy [83, 84]. A parallel magnetic field alters electron states such that everywhere except a small magnetic field range,

$$\Delta_{SAS} \sim \frac{1}{c}\, dBv_F,$$

where Δ_{SAS} is the tunnel energy, i.e., the boundary excitations of the continuum occur as interlayer ones [78]. The critical magnetic field in which the energy of single-particle excitations achieves an extremum is not defined by relation (15) but vanishes.

We compare the critical magnetic fields for single and double-layer systems as functions of the dipole moment in a zero magnetic field. In the former system, the dipole moment decreases with decreasing the width of the quantum well (Fig. 14). In a DQW, the dipole moment decreases upon symmetrization. Single- and double-layer systems differ in terms of the action of the magnetic field on electron states in the two lowest dimensionally quantized subbands. The magnetic field in a double-layer system alters wave functions but has virtually no effect on them in a single-layer one. As a result, the critical magnetic field is inversely proportional to the dipole moment for single-layer system (15) and tends to zero when a double-layer system undergoes symmetrization. Therefore, if the DQW is to be transferred to the symmetric state, a finite momentum must be transmitted to single-particle electron excitations and the system must be balanced until the excitation energy persists despite the magnetic field inversion. The accuracy of this method is determined by the relation between the line widths of inelastic light scattering and the tunnel energy. It was estimated in experiments that balancing DQWs is feasible at the tunnel energies up to 0.1 meV [78].

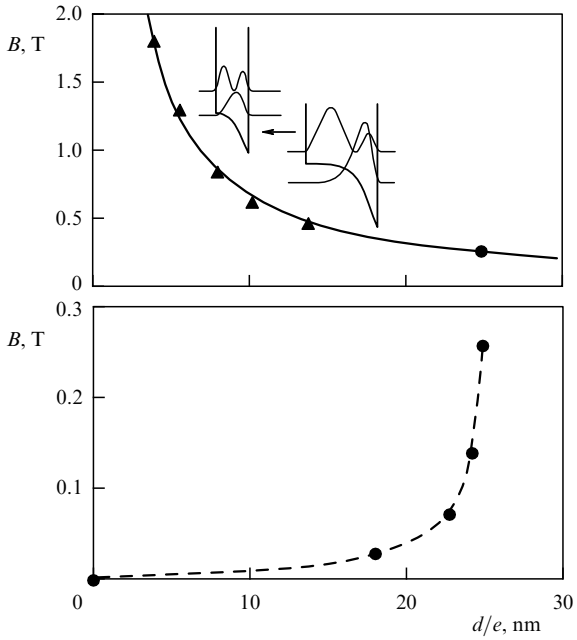

Figure 14. Experimental critical magnetic field as a function of the theoretical dipole moment of single-particle excitations (14) for single (triangles) and double (circles) quantum wells. The inset schematically shows the results of self-consistent calculations of the limiting potential profile of single quantum wells and the squared electron wave functions in the first two dimensionally quantized subbands for the widest and the narrowest quantum wells; the solid line is the calculated critical magnetic field $B = qc/d$.

5.2 Plasma excitations in double quantum wells

The above balance method was used to study plasma modes in symmetric and asymmetric DQW states and their modification during transition from a symmetric state to an asymmetric one (Fig. 15). A characteristic feature of the symmetric state is the absence in the spectrum of a gapless plasma mode with the linear dispersion law or an acoustic plasmon, i.e., out-of-phase oscillation of the charge density in symmetric and asymmetric subbands [79, 85]. The energy of the acoustic plasmon is determined by the difference between the intra- and intersubband of Coulomb interactions of electrons. The electron density distributions in two subbands of a symmetric DQW almost coincide, and therefore the acoustic plasmon mode is smoothed and falls into into the continuum of single-particle excitations.

The acoustic plasmon is replaced by a tunnel one, which is a gap mode with linear dispersion in the longwave limit ($qa_B \ll 1$) (Fig. 16). The linear slope is close to that of the acoustic plasmon in an asymmetric DQW with the same parameters (the total electron density and interwell distance). This property of the tunnel plasmon was a source of gross theoretical mistakes [86–89]. It was supposed that the tunnel plasmon is not a separate plasma mode but an acoustic plasmon mode with the opening longwave plasma gap.

Indeed, the two plasma modes of totally different nature, tunnel and acoustic, display linear dispersion dependences with the slopes equalized as the tunnel coupling decreases. Moreover, the cross sections of inelastic light scattering from the tunnel plasmon in the symmetric state and the acoustic one in the asymmetric state coincide (Fig. 17). Because the cross section is proportional to the dynamic structural factor, the distributions of charge fluctuations in the tunnel and acoustic plasma modes are identical. It can be concluded that the tunnel plasmon is an out-of-phase excitation of the electron density in two DQW layers. As the tunnel gap increases ($\Delta_{SAS} \sim qv_F$), the cross section of the tunnel plasmon decreases and the longwave dispersion flattens [90]. In this limit, the energy of electron transverse oscillations

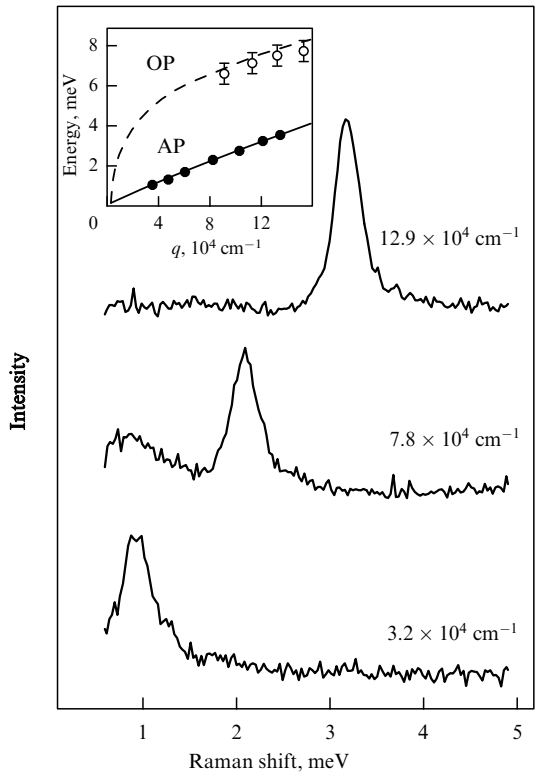

Figure 15. Inelastic light scattering spectra of an acoustic plasmon in a double quantum well in the asymmetric state at different momentum values. The inset shows dispersion dependences of acoustic (AP) and optical (OP) plasmons, found experimentally (dots) and calculated in the framework of classical electrodynamics.

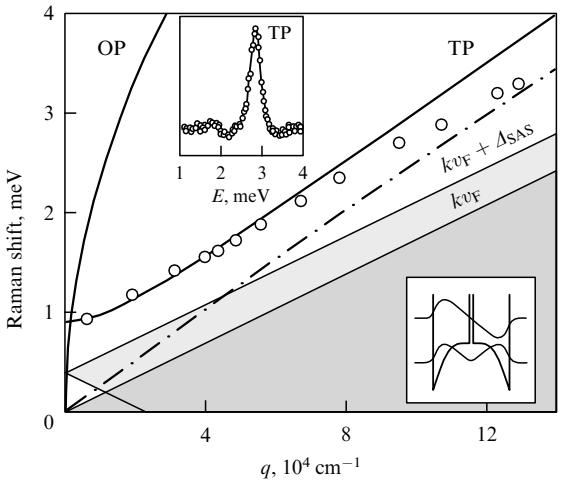

Figure 16. Dispersion dependences of tunnel (TP) and optical (OP) plasmons found experimentally (circles) and calculated in the random-phase approximation (solid lines). Shaded areas are intra- and intersubband continua of single-particle excitations. The dash-dotted line represents the dispersion dependence of the acoustic plasmon in the asymmetric state. The insets demonstrate the spectrum of inelastic light scattering from the tunnel plasmon and the profile of the double quantum well potential with envelopes of wave functions in the symmetric and asymmetric subbands of dimensional quantization.

exceeds the kinetic energy in the plane and the tunnel plasmon becomes a collective mode of the exciton type.

Inelastic light scattering spectra contain an optical plasmon, besides a tunnel one, whose energy is only weakly

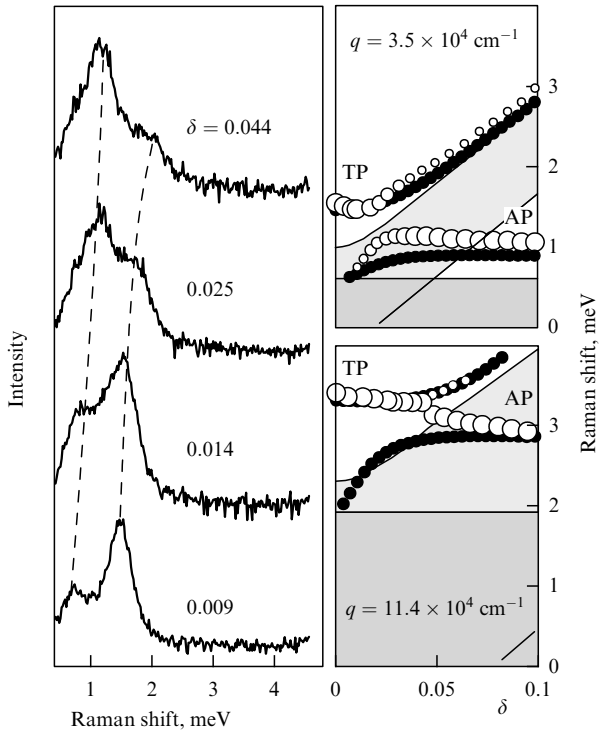

Figure 17. Variation of inelastic light scattering spectra depending on the degree of asymmetry of the double quantum well (left) and on the energy of tunnel and acoustic plasmons for two momentum values depending on the degree of asymmetry of the double quantum well (right); white circles — experimental data, black circles — calculation in the random-phase approximation. The size of the experimental points is proportional to the cross section of inelastic light scattering. Shaded areas are intra- and intersubband continua of single-particle excitations. The degree of skewness $\delta = (N_1 - N_2)/(N_1 + N_2)$ determines the electric field imbalance on two sides of the DQW.

dependent on the tunnel coupling. The difference of tunneling effects on the tunnel and optical plasma modes may be interpreted as follows. In the case of in-phase oscillations of the electron density in two subbands and layers, there is an equal probability of electron tunneling from each layer to its counterpart; therefore, tunneling does not considerably influence in-phase oscillations. In the tunnel mode, charge fluctuations in the two layers have opposite signs and hence different probabilities of tunneling in different layers. Electrons travel not only in the plane of the layers but also across it, which accounts for a change in the tunnel plasmon energy.

The transition from the symmetric state to the asymmetric one is accompanied by a decrease in the tunnel plasmon scattering cross section, and the plasmon itself decays into intersubband one-particle excitations. In contrast, the energy of the acoustic plasmon increases and may exceed the boundary energy of the single-particle continuum at a certain degree of the DQW skewness. Thus, a DQW with the tunnel coupling involves a skewness such that the spectrum contains two out-of phase weakly decaying plasma modes (Fig. 17). There is a phase transition from the symmetric to the asymmetric state when the tunnel coupling tends to zero. The tunnel plasmon exists only in the symmetric phase and the acoustic plasmon in the asymmetric one; the two plasma modes do not occur simultaneously.

We note that acoustic and tunnel plasmons are totally different oscillations, the former being an intrasubband

oscillation and the latter an intersubband one associated with electron transitions between the lowest subbands of dimensional quantization. Physical properties of tunnel and acoustic plasmons are identical only in the weak-tunneling limit. In the opposite limit, the tunnel plasmon is an exciton-type excitation with a quadratic dispersion dependence. In contrast, the acoustic plasmon shows a linear dispersion dependence virtually unrelated to the tunnel gap size.

5.3 Magnetoplasma excitations in double quantum wells

We consider a modification of the intersubband excitation spectrum in DQWs in a perpendicular magnetic field. The simplest case is represented by an asymmetric DQW in which collective excitations are acoustic and optical plasmons.

Acoustic and optical plasmons are transformed by the magnetic field into hybrid magnetoacoustic and magnetooptic plasma modes, respectively, in which electrons are simultaneously involved in plasma and cyclotron oscillations. Their energies are expressed in the framework of classical electrodynamics as

$$\omega^2(k) = \omega_c^2 + \omega_{AP,\,OP}^2(q)\,, \tag{17}$$

where $\omega_{AP,\,OP}^2(q)$ are the plasma frequencies of acoustic and optical plasmons without a magnetic field with the momentum $q = k$ (8) [79]. This expression is in good agreement with experiment (Fig. 18). Both magnetoplasma modes interact with intrasubband Bernstein modes, with two types of the Bernstein modes being observed under experimental conditions. These modes with the same index can interact with either an optical or an acoustic plasmon, and the energies of the corresponding hybrid plasma-Bernstein modes anticross with each other [80]. The energies of the two Bernstein modes coincide outside the resonance area.

Inelastic light scattering spectra in the magnetic field of symmetric and asymmetric DQWs in the weak-tunneling limit virtually coincide due to the similar physical properties of acoustic and tunnel plasmons. The place of the magnetoacoustic plasmon is taken by the magnetotunnel plasmon associated with electron transitions from the upper filled Landau level of the symmetric dimensionally quantized subband with a number n to the unfilled Landau level with the number $n+1$ of the antisymmetric subband. The difference between the energies of magnetoacoustic and magnetotunnel plasmons is determined by the tunnel gap, which is small in the weak-tunneling limit.

The magnetoexcitation spectrum also shows an exciton-type mode with the energy exceeding the tunnel gap by the depolarization shift,

$$\omega^2 = \Delta_{SAS}^2 + \frac{2\sqrt{2\pi}e^2L}{\varepsilon}\,(n_1 - n_2)\,\Delta_{SAS}\,, \tag{18}$$

where L is the parameter characterizing nonlocality of the electron wave function in each well [34]. This mode is analogous with the intersubband singlet magnetoexciton in single quantum wells, and its energy is independent of the magnetic field. In the strong-tunneling limit $\Delta_{SAS} \sim E_F$, the DQW magnetoexcitation spectrum is similar to the spectrum of intersubband magnetoexcitations of single quantum wells and the inelastic light spectra are dominated by the exciton-type mode.

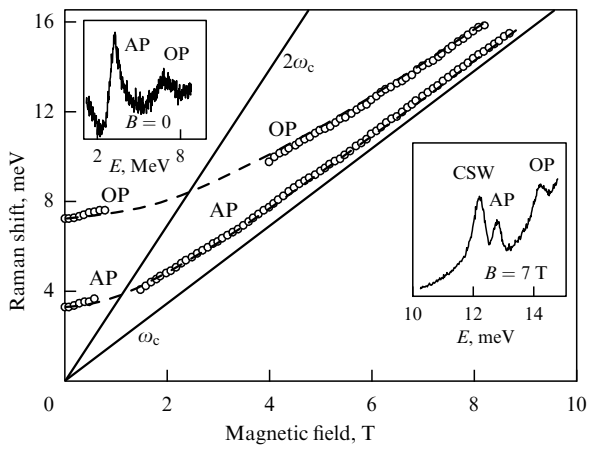

Figure 18. Magnetofield dependences of the energies of magnetoacoustic (AP) and magnetooptic (OP) plasmons. Solid lines — multiple cyclotron energies, dashed lines — dependences $\omega(k) = (\omega_c^2 + \omega_{AP,\,OP}^2(q))^{1/2}$. The insets schematically represent characteristic spectra of inelastic light scattering at $B = 0$ and $B = 7$ T.

6. Conclusion

This review was aimed at discussing intersubband and cyclotron branches of collective excitations and magnetoexcitations, which by no means exhaust the diversity of possible degrees of freedom of a strongly correlated 2D electron system. For example, neither intralevel excitations in fractional QHE states nor excitations in a system of composite fermions were considered. Recent research in these areas has demonstrated a marked discrepancy between the energy of cyclotron resonance on composite fermions and the energies of supraliquid excitations obtained by the inelastic light scattering technique [91, 92]. The nature of this discordance remains to be clarified.

Another important problem is the appearance of so-called 'magnetotron' resonances in experiments on inelastic light scattering [93, 94]. Attempts to ascribe them to processes resulting from gross violation of the momentum conservation law have not been confirmed by theoretical calculations and experiments on superhigh-quality quantum wells with the electron mobility up to 2×10^7 cm^2 V^{-1} s^{-1} [58]. Studies of inelastic light scattering on the Goldstone mode in the ferromagnetic state $\nu = 1$ have thus far been hampered by the poor quality of heterostructures with double quantum wells. Further progress in the technology for obtaining heterostructures with single and double quantum wells may be instrumental in resolving these experimental problems.

References

1. Landau L D *Zh. Eksp. Teor. Fiz.* **11** 592 (1941)
2. Bohm D, Pines D *Phys. Rev.* **82** 625 (1951); Pines D, Bohm D *Phys. Rev.* **85** 338 (1952)
3. Stern F *Phys. Rev. Lett.* **18** 546 (1967)
4. Kukushkin I V et al. *Phys. Rev. Lett.* **90** 156801 (2003)
5. Dahl D A, Sham L J *Phys. Rev. B* **16** 651 (1977)
6. Grimes C C, Adams G *Phys. Rev. Lett.* **36** 145 (1976)
7. Allen S J (Jr), Tsui D C, Logan R A *Phys. Rev. Lett.* **38** 980 (1977)
8. Theis T N, Kotthaus J P, Stiles P J *Solid State Commun.* **26** 603 (1978)
9. Ando T, Fowler A B, Stern F *Rev. Mod. Phys.* **54** 437 (1982)
10. v. Klitzing K, Dorda G, Pepper M *Phys. Rev. Lett.* **45** 494 (1980)
11. Tsui D C, Stormer H L, Gossard A C *Phys. Rev. Lett.* **48** 1559 (1982)
12. Tsui D C et al. *Phys. Rev. B* **28** 2274 (1983)

13. Chang A M et al. *Phys. Rev. B* **28** 6133 (1983)
14. Laughlin R B *Phys. Rev. Lett.* **50** 1395 (1983)
15. Jain J K *Phys. Rev. Lett.* **63** 199 (1989); *Phys. Rev. B* **41** 7653 (1990); Jain J K, Kamilla R K, in *Composite Fermions: a Unified View of the Quantum Hall Regime* (Ed. O Heinonen) (Singapore: World Scientific, 1998) p. 1
16. Lopez A, Fradkin E *Phys. Rev. B* **44** 5246 (1991); **47** 7080 (1993); *Phys. Rev. Lett.* **69** 2126 (1992)
17. Halperin B I, Lee P A Read N *Phys. Rev. B* **47** 7312 (1993)
18. Shankar R *Phys. Rev. B* **63** 085322 (2001)
19. Kallin C, Halperin B I *Phys. Rev. B* **30** 5655 (1984)
20. Lamb W E (Jr) *Phys. Rev.* **85** 259 (1952); Gor'kov L P, Dzyaloshinskii I E *Zh. Eksp. Teor. Fiz.* **53** 717 (1967) [*Sov. Phys. JETP* **26** 449 (1967)]
21. Johnson B R, Hirschfelder J O, Yang K-H *Rev. Mod. Phys.* **55** 109 (1983)
22. Lerner I V, Lozovik Yu E *Zh. Eksp. Teor. Fiz.* **78** 1167 (1980) [*Sov. Phys. JETP* **51** 588 (1980)]
23. Pinczuk A et al. *Phys. Rev. Lett.* **68** 3623 (1992)
24. Kohn W *Phys. Rev.* **123** 1242 (1961)
25. Sondhi S L et al. *Phys. Rev. B* **47** 16419 (1993)
26. Comtet A et al. (Eds) *Aspects Topologiques de la Physique en Basse Dimension. Topological Aspects of Low Dimensional Systems* (Les Houches — Ecole d'Ete de Physique Theorique, Vol. 69) (Berlin: Springer, 1999)
27. Willett R L et al. *Phys. Rev. B* **37** 8476 (1988)
28. Pinczuk A et al. *Phys. Rev. Lett.* **70** 3983 (1993)
29. Gramila T J et al. *Phys. Rev. Lett.* **66** 1216 (1991)
30. Yoshioka D, MacDonald A H, Girvin S M *Phys. Rev. B* **39** 1932 (1989)
31. Platzman P M, Lenosky T *Phys. Rev. B* **52** 10327 (1995)
32. Oji H C A, MacDonald A H, Girvin S M *Phys. Rev. Lett.* **58** 824 (1987)
33. Bertoni A et al. *Phys. Rev. Lett.* **84** 5912 (2000)
34. Vitlina R Z, Chaplik A V *Zh. Eksp. Teor. Fiz.* **81** 1011 (1981) [*Sov. Phys. JETP* **54** 536 (1981)]
35. Das Sarma S, Madhukar A *Phys. Rev. B* **23** 805 (1981)
36. Fasol G et al. *Phys. Rev. B* **39** 12695 (1989)
37. Bhatti A S et al. *Phys. Rev. B* **51** 2252 (1995); Kainth D S et al. *Phys. Rev. B* **57** R2065 (1998)
38. Eisenstein J P et al. *Phys. Rev. Lett.* **68** 1383 (1992)
39. Suen Y W et al. *Phys. Rev. Lett.* **68** 1379 (1992)
40. Rezayi E H, Haldane F D M *Bull. Am. Phys. Soc.* **32** 892 (1987)
41. Chakraborty T, Pietiläinen P *Phys. Rev. Lett.* **59** 2784 (1987)
42. Fertig H A *Phys. Rev. B* **40** 1087 (1989)
43. Kellogg M et al. *Phys. Rev. Lett.* **93** 036801 (2004)
44. Wen X-G, Zee A *Phys. Rev. Lett.* **69** 1811 (1992); *Phys. Rev. B* **47** 2265 (1993)
45. Ezawa Z F, Iwazaki A *Phys. Rev. B* **47** 7295 (1993); *Phys. Rev. Lett.* **70** 3119 (1993); *Phys. Rev. B* **48** 15189 (1993)
46. Abstreiter G, Cardona M, Pinczuk A, in *Light Scattering in Solid IV* (Topics in Applied Physics, Vol. 54, Ed. M Cardona, G Güntherodt) (Berlin: Springer-Verlag, 1984) p. 5
47. Kukushkin I V, Timofeev V B *Adv. Phys.* **45** 147 (1996)
48. Kulik L V et al. *Phys. Rev. B* **63** 201402 (2001)
49. Kulik L V et al. *Pis'ma Zh. Eksp. Teor. Fiz.* **74** 300 (2001) [*JETP Lett.* **74** 270 (2001)]
50. Kulik L V et al. *Phys. Rev. B* **72** 073304 (2005)
51. Summers G M et al. *Phys. Rev. Lett.* **70** 2150 (1993); Besson M et al. *Semicond. Sci. Technol.* **7** 1274 (1992)
52. Finkelstein G, Shtrikman H, Bar-Joseph I *Phys. Rev. Lett.* **74** 976 (1995)
53. Feynman R P *Statistical Mechanics* (Reading Mass.: Benjamin, 1972) Ch. 11 [Translated into Russian (Moscow: Mir, 1978) Ch. 11]
54. Girvin S M, MacDonald A H, Platzman P M *Phys. Rev. Lett.* **54** 581 (1985); *Phys. Rev. B* **33** 2481 (1986)
55. MacDonald A H, Oji H C A, Girvin S M *Phys. Rev. Lett.* **55** 2208 (1985)
56. Longo J P, Kallin C *Phys. Rev. B* **47** 4429 (1993)
57. Oji H C A, MacDonald A H *Phys. Rev. B* **33** 3810 (1986)
58. Kallin C, Halperin B I *Phys. Rev. B* **31** 3635 (1985)
59. Dickmann S, Kukushkin I V *Phys. Rev. B* **71** 241310(R) (2005)
60. Kirpichev V E et al. *Phys. Rev. B* **59** R12751 (1999)
61. Kulik L V et al. *Phys. Rev. Lett.* **86** 1837 (2001)
62. Kulik L V et al. *Phys. Rev. B* **61** 12717 (2000)
63. Kulik L V et al. *Zh. Eksp. Teor. Fiz.* **122** 1074 (2002) [*JETP* **95** 927 (2002)]
64. Kulik L V et al. *Phys. Rev. B* **61** 1712 (2000); **66** 073306 (2002)
65. Tselis A C, Quinn J J *Phys. Rev. B* **29** 3318 (1984)
66. Pinczuk A et al. *Phys. Rev. Lett.* **63** 1633 (1989)
67. Gammon D et al. *Phys. Rev. Lett.* **68** 1884 (1992)
68. Ernst S et al. *Phys. Rev. Lett.* **72** 4029 (1994)
69. Ando T *Phys. Rev. B* **19** 2106 (1979)
70. Batke E, Weimann G, Schlapp W *Phys. Rev. B* **43** 6812 (1991)
71. Brozak G et al. *Phys. Rev. B* **47** 9981 (1993)
72. Bisti V E *Pis'ma Zh. Eksp. Teor. Fiz.* **69** 543 (1999) [*JETP Lett.* **69** 584 (1999)]
73. Bisti V E *Pis'ma Zh. Eksp. Teor. Fiz.* **73** 25 (2001) [*JETP Lett.* **73** 21 (2001)]
74. Marmorkos I K, Das Sarma S *Phys. Rev. B* **48** 1544 (1993)
75. Wendler L, Pechstedt R *J. Phys: Condens. Matter* **2** 8881 (1990)
76. Avron J E, Herbst I W, Simon B *Ann. Phys.* (New York) **114** 431 (1978)
77. Tovstonog S V et al. *Pis'ma Zh. Eksp. Teor. Fiz.* **78** 1151 (2003) [*JETP Lett.* **78** 654 (2003)]
78. Kulik L V et al. *Phys. Rev. B* **71** 165303 (2005)
79. Kulik L V et al. *Phys. Rev. B* **70** 033304 (2004)
80. Tovstonog S V et al. *Phys. Rev. B* **66** 241308 (2002); *Pis'ma Zh. Eksp. Teor. Fiz.* **76** 592 (2002) [*JETP Lett.* **76** 511 (2002)]
81. Tovstonog S V et al. *Pis'ma Zh. Eksp. Teor. Fiz.* **79** 54 (2004) [*JETP Lett.* **79** 48 (2004)]
82. Jain J K, Das Sarma S *Phys. Rev. B* **36** 5949 (1987)
83. Gumbs G, Aïzin G R *Phys. Rev. B* **51** 7074 (1995)
84. Gorbatsevich A A, Tokatly I V *Semicond. Sci. Technol.* **13** 288 (1998)
85. Bootsmann M-T et al. *Phys. Rev. B* **67** 121309(R) (2003)
86. Aïzin G R, Gumbs G *Phys. Rev. B* **54** 2049 (1996)
87. Reboredo F A, Proetto C R *Phys. Rev. Lett.* **79** 463 (1997)
88. Bolcatto P G, Proetto C R *Phys. Rev. Lett.* **85** 1734 (2000)
89. Das Sarma S, Hwang E H *Phys. Rev. Lett.* **81** 4216 (1998)
90. Decca R et al. *Phys. Rev. Lett.* **72** 1506 (1994)
91. Kukushkin I V et al. *Nature* **415** 409 (2002)
92. Kang M et al. *Phys. Rev. Lett.* **84** 546 (2000)
93. Pinczuk A et al. *Phys. Rev. Lett.* **61** 2701 (1988)
94. Luin S et al. *Phys. Rev. Lett.* **90** 236802 (2003)